Available online at www.sciencedirect.com
ScienceDirect
Journal of Hazardous Materials 144 (2007) 93–100
Journal of Hazardous Materials
www.elsevier.com/locate/jhazmat

Adsorption of reactive dye onto carbon nanotubes: Equilibrium, kinetics and thermodynamics

Chung-Hsin Wu *

Department of Environmental Engineering, Da-Yeh University, 112 Shan-Jiau Road, Da-Tsuen, Chang-Hua, Taiwan, ROC

Received 15 August 2006; received in revised form 25 September 2006; accepted 28 September 2006
Available online 1 October 2006

Abstract

The adsorption efficiency of carbon nanotubes for Procion Red MX-5B at various pHs and temperatures was examined. The amount adsorbed increased with the CNTs dosage; however, the adsorption capacity initially increased with the CNTs dosage (<0.25 g/l) and then declined as the CNTs dosage increased further (>0.25 g/l). The linear correlation coefficients and standard deviations of Langmuir and Freundlich isotherms were determined and the results revealed that Langmuir isotherm fitted the experimental results well. Kinetic analyses were conducted using pseudo first- and second-order models and the intraparticle diffusion model. The regression results showed that the adsorption kinetics were more accurately represented by a pseudo second-order model. Changes in the free energy of adsorption (ΔG°), enthalpy (ΔH°) and entropy (ΔS°), as well as the activation energy (E_a) were determined. ΔH° and ΔS° were 31.55 kJ/mol and 216.99 J/mol K, respectively, at pH 6.5 and 41.47 kJ/mol and 244.64 J/mol K at pH 10. The activation energy was 33.35 kJ/mol at pH 6.5. ΔH°, ΔG° and E_a all suggested that the adsorption of Procion Red MX-5B onto CNTs was by physisorption.

Keywords: Adsorption; Carbon nanotubes; Isotherm; Kinetics; Thermodynamics

1. Introduction

Dyes are used extensively in the textile, leather, paper, plastic and other industries. Reactive dye production is characterized by the great losses that are caused by the high solubility of the dyes, which also creates an economical and environmental problem. Removing reactive dyes by coagulation is difficult because the dyes are highly soluble in water. Hence, the removal of dye from colored reactive dye wastewater is an important environmental issue. Adsorption has been found to be superior to other techniques for treating wastewater: it is low-cost, highly efficient, simple, easy to perform and insensitive to toxic substances. Moreover, liquid-phase adsorption has been demonstrated to be highly efficient in removing dyes from waste effluent. Hence, adsorption was selected herein as the approach used to treat reactive dye wastewater.

Carbon nanotubes (CNTs) are attracting increasing research interest as a new adsorbent. They are an attractive alternative for the removal of organic and inorganic contaminants from water, because they have a large specific surface area, small size, and hollow and layered structures. Recently, CNTs have been found to be efficient adsorbents with a capacity that exceeds that of activated carbon [1,2]. Much attention has been paid to the adsorption by CNTs such as ZnP^{2+} [2], CdP^{2+} [3], PbP^{2+} [4–7], CuP^{2+} [7], CrP^{6+} [8], fluoride [9], arsenate [10], trihalomethanes [11], 1,2-dichlorobenzeze [12] and dioxin [1]. Experimental results demonstrate that compared with activated carbon (AC), CNTs comparatively improve adsorption of Procion Red MX-5B onto TiO_2; the saturation adsorption capacity of TiO_2, TiO_2/AC and TiO_2/CNTs is 6.3, 13.3 and 14.2 mg/g, respectively [13]. Furthermore, Yu et al. [14] indicated that TiO_2/CNTs composites have higher photocatalytic activity than TiO_2 and the TiO_2/AC composite. Earlier investigations have suggested that CNTs may be a promising adsorbents for treating wastewater. However, few studies have been conducted on the adsorption of organic pollutants by CNTs, except for dioxin [1]; trihalomethanes [11] and 1,2-dichlorobenzene [12]. The reactive dye, Procion Red MX-5B, was employed as the organic pollutant to be treated by CNTs in this work.

* Tel.: +886 5 5347311; fax: +886 5 5334958.
E-mail address: chunghsinwu@yahoo.com.tw.

0304-3894/$ – see front matter © 2006 Elsevier B.V. All rights reserved.
doi:10.1016/j.jhazmat.2006.09.083

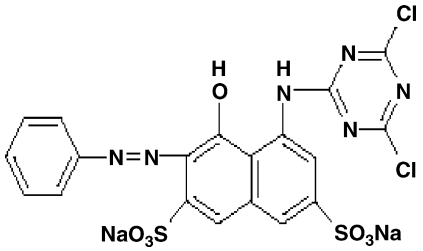

Fig. 1. The structure of Procion Red MX-5B.

An understanding of adsorption equilibrium, kinetics and thermodynamics is critical in supplying the basic information required for the design and operation of adsorption equipment. Earlier studies have obtained only equilibrium and kinetic adsorption data and few works have measured the thermodynamic parameters of adsorption on CNTs: Peng et al. [12] measured those of the adsorption of 1,2-dichlorobenzene and Li et al. [5] examined the thermodynamics of the adsorption of PbP^{2+} on CNTs. Few investigations focused on the adsorption of organic pollutants on CNTs and simultaneously determined the equilibrium, kinetics and thermodynamic parameters. Hence, this study elucidates the equilibrium, kinetics and thermodynamics of the adsorption of Procion Red MX-5B onto CNTs. The Langmuir and Freundlich equations were used to fit the equilibrium data. The effects of temperature on the dynamic behaviors of adsorption were determined. The adsorption rates were determined quantitatively and those obtained using the pseudo first- and second-order models and the intraparticle diffusion model was also compared. The objectives of this study were: (i) to determine the appropriate CNTs dosage to adsorb Procion Red MX-5B; (ii) to measure the coefficients of Langmuir and Freundlich isotherms; (iii) to evaluate the adsorption rate using various kinetic models; (iv) to derive the thermodynamic parameters—activation energy (E_a), and the changes in free energy (ΔG°), enthalpy (ΔH°) and entropy (ΔS°) during adsorption at various pH values.

2. Materials and methods

2.1. Materials

The CNTs adopted herein were multi-wall nanotubes (CBT, MWNTs-2040, which were used without further purification). CNTs were produced by the pyrolysis of methane gas on particles of Ni in a chemical vapor deposition. The length of CNTs was 5–15 μm and the mass proportion of amorphous carbon in CNTs was less than 2%. The parent compound, Procion Red MX-5B, was purchased from Aldrich Chemical Company. The formula, molecular weight and maximum wavelength of light absorbed by Procion Red MX-5B (CI Reactive Red 2) were $C_{19}H_{10}Cl_2N_6Na_2O_7S_2$, 615 g/mol, and 538 nm, respectively. The structure of Procion Red MX-5B is shown in Fig. 1. All solutions were prepared using deionized water (Milli-Q) and reagent-grade chemicals.

2.2. Characterization of CNTs

CNTs were subjected to energy dispersive spectrometer for surface distribution of elemental composition and scanning electron microscopy (SEM) with a JEOL JSM-6500F. Size and morphology of CNTs were recorded by transmission electron microscopy (TEM) with a Philips/FEI Tecnai 20 G2 S-Twin. The specific surface area of CNTs was measured by the BET method using a Quantachrome-Autosorb1. The zeta potential of the CNTs was measured at pH values of 2–9 using a Zeta-Meter 3.0. Ten measurements were made of each sample at each pH and the average was determined as the zeta potential.

2.3. Adsorption experiments

All experiments were conducted in a closed 250 ml glass pyramid bottle and $HClO_4$ or NaOH was used to adjust the pH. The 250 ml glass pyramid bottle, containing 0.05 g of CNTs and 200 ml of Procion Red MX-5B solution, was placed in a water bath and shaken at 160 rpm. In experiments to determine CNTs dosage, Procion Red MX-5B (20 mg/l) was equilibrated with a suspension of CNTs (0.025, 0.05, 0.25, 0.5 and 0.75 g/l) at pH 6.5 for 24 h. In the experiments on the effect of temperature (Procion Red MX-5B = 20 mg/l and CNTs = 0.25 g/l), the temperature was held at 281, 291, 301 and 321 K and the pH was fixed at 6.5 and 10. At the end of the equilibrium period, the suspensions were centrifuged at 4000 rpm for 10 min, and the supernatant was then filtered through 0.2 μm filter paper (Gelman Sciences) for later analysis of the dye concentration. The adsorption of Procion Red MX-5B was detected using a spectrophotometer (Hitachi-U2001) at 538 nm. Each experiment was performed twice and experimental results are average values. The adsorbed amounts q_i were calculated from:

$$q_i = \frac{C_i - C_o}{m} \quad (1)$$

where C_i and C_o are the initial and equilibrium concentrations, respectively, in mg/l, and m is the amount of CNTs in g/l.

3. Results and discussion

3.1. Effects of CNTs dosage

Fig. 2 displays the surface morphology of CNTs. The SEM and TEM figures show that the CNTs were cylindrical and that the range of main external and internal diameters was 20–80 and 5–10 nm, respectively. Additionally, the distance between the wall and wall of CNTs was approximately 0.5–1 nm and the TEM analysis confirmed the hollow structure of CNTs. The specific surface area of the CNTs used in this study was 106.9 m^2/g. The pH of the zero point of charge (pH_{zpc}) for CNTs was determined to be 4.9, which was the same as that measured by Lu and Chiu [2] for multi-wall nanotubes. This result indicated that the surface of CNTs was positively charged at a solution pH of <4.9. The element characteristics of CNTs showed the content of C, O and Ni was 90.6, 8.1 and 1.3%, respectively. Since the CNTs were generated by the pyrolysis of methane gas on particles of

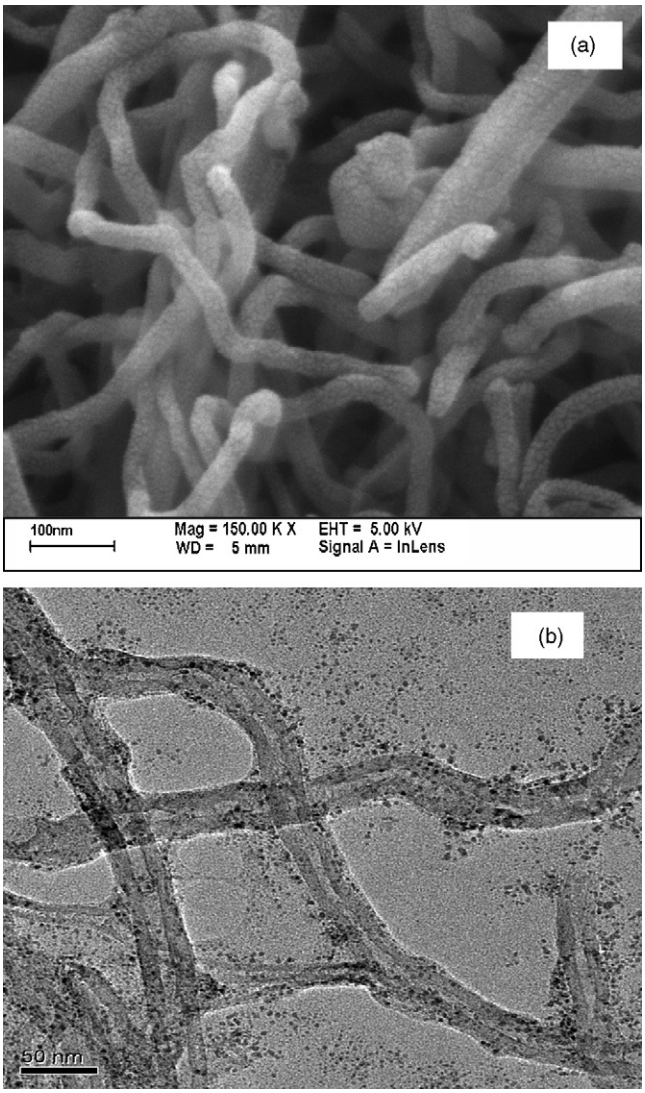

Fig. 2. Micrographs of CNTs (a) SEM and (b) TEM.

Ni by chemical vapor deposition, the major element was carbon, with only a few Ni atoms present.

Fig. 3 presents the effect of CNTs dosage on the adsorption of Procion Red MX-5B. The amount adsorbed increased with the dose of CNTs; however, the adsorption capacity initially increased and then dropped as the CNTs dosage increased. In dilute CNTs suspensions (<0.25 g/l), CNTs are suggested to be separated and dispersed. In this case, the adsorption capacity at the external surface predominated, and for this reason, the adsorption capacity of Procion Red MX-5B would be high. Increasing the CNTs dose (>0.25 g/l) increases the probability of the CNTs entanglement in the solution, causing adsorption in the interlayer space and a decrease in the aggregation of dye at the external surface.

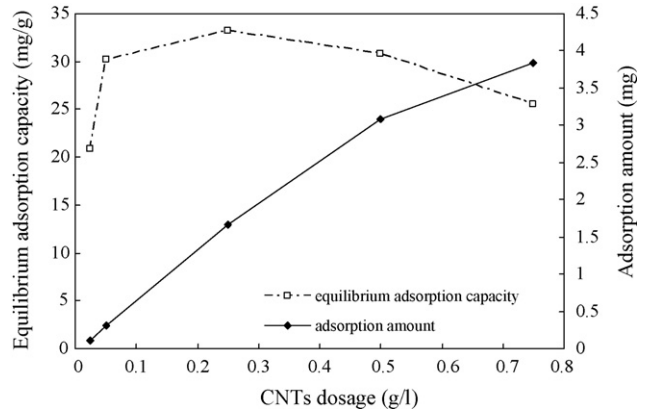

Fig. 3. Effect of CNTs dosage on the adsorption of Procion Red MX-5B (Procion Red MX-5B = 20 mg/l, pH 6.5, contact time = 24 h and T = 301 K).

Accordingly, the adsorption capacity declined as the CNTs dosage increased above 0.25 g/l. Moreover, the high CNTs dosage may influence the physical characteristics of the solid–liquid suspensions, such as by increasing the viscosity and inhibiting the diffusion of dye molecules to the surface of the CNTs. Since the concentration of Procion Red MX-5B was fixed, the adsorption capacity decreased as the CNTs dosage increased (>0.25 g/l). The increase with CNTs dosage of the amount of dye adsorbed was caused by the availability of more surface area of the CNTs. Direct evidence of CNTs entanglement was unclear and unobtainable. However, similar observations can be found in literature. Bhattacharyya and Sharma [15], who utilized Neem leaf powder to adsorb dyes, suggested that the amount adsorbed (mg/g) decreased as the amount of the adsorbent increased; similar results were also obtained for algae cell walls by Marungrueng and Pavasant [16] and for cross-linked chitosan beads by Chiou et al. [17]. Gemeay [18] employed Na^+-montmorillonite to adsorb rhodamine-6G and obtained similar results to those in this study: adsorption increased as Na^+-montmorillonite increased (<0.2 g/l) and decreased with further increases of Na^+-montmorillonite (>0.2 g/l). Since the adsorption capacity was greatest when 0.25 g/l CNTs was added, this dosage (0.25 g/l) was used in the following experiments.

3.2. Adsorption isotherms

The correlation of equilibrium adsorption data by either theoretical or empirical equations is important in the design and operation of adsorption systems. This study employed the Langmuir and Freundlich models to describe the equilibrium adsorption. The expression of the Langmuir model is:

$$q = q_m \frac{K_L C}{1 + K_L C} \tag{2}$$

where q is the amount of dye adsorbed per gram of CNTs (mg/g); C denotes the equilibrium concentration of dye in solution (mg/l); K_L represents the Langmuir constant (l/mg) that relates to the affinity of binding sites and q_m is the theoretical saturation capacity of the monolayer (mg/g). The values of q_m and K_L are calculated from the intercept and slope of the linear plot of $1/q$ versus $1/C$. Furthermore, the effect of the isotherm shape is considered with a view to predict whether an adsorption system is favorable or unfavorable. Another important parameter, R_L, called the separation factor or equilibrium parameter, also evaluated in this study, is determined from the relation:

$$R_L = \frac{1}{1 + K_L C_0} \tag{3}$$

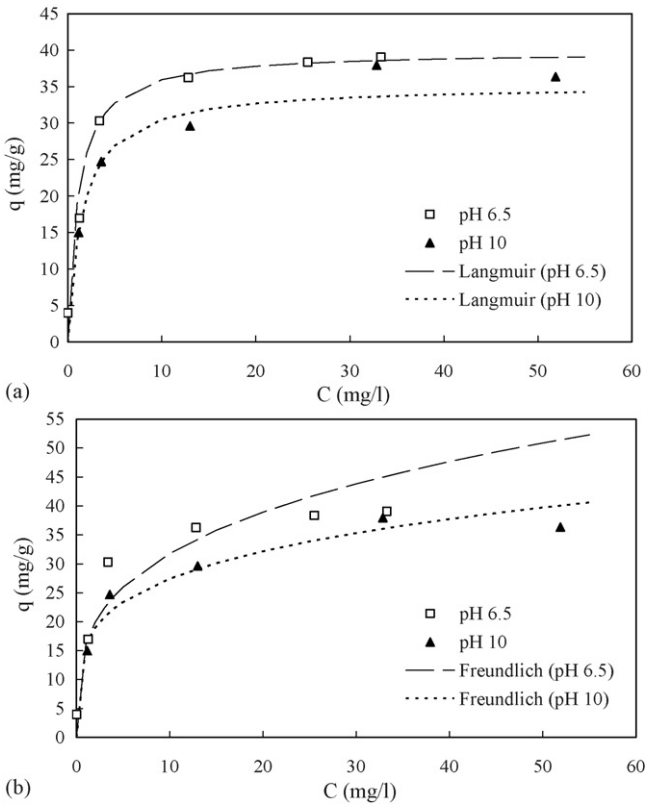

Fig. 4. Adsorption isotherms of Procion Red MX-5B: (a) Langmuir plots and (b) Freundlich plots (CNTs = 0.25 g/l, contact time = 24 h and T = 301 K).

where K_L is the Langmuir constant (l/mg) and C_0 is the initial dye concentration (20 mg/l). Ho and McKay [19] established that (i) $0 < R_L < 1$ for favorable adsorption, (ii) $R_L > 1$ for unfavorable adsorption, (iii) $R_L = 1$ for linear adsorption and (iv) $R_L = 0$ for irreversible adsorption.

The Freundlich model is an empirical equation that assumes heterogeneous adsorption due to the diversity of adsorption sites. The Freundlich equation is:

$$q = K_F C^{1/n} \quad (4)$$

where q is the equilibrium dye concentration on CNTs (mg/g); C the equilibrium dye concentration in solution (mg/l); K_F and n are the Freundlich constants, which represent the adsorption capacity and the adsorption strength, respectively. K_F and $1/n$ can be obtained from the intercept and slope of the linear plot of $\ln(q)$ versus $\ln(C)$. The magnitude of $1/n$ quantifies the favorability of adsorption and the degree of heterogeneity of the CNTs surface. If $1/n$ is less than unity, indicating favorable adsorption, then the adsorption capacity increases and new adsorption sites occur [20]. The validity of models was determined by calculating the standard deviation (S.D., %) using:

$$\text{S.D.} = \sqrt{\frac{\sum[(q_{exp} - q_{cal})/q_{exp}]^2}{n-1}} \times 100 \quad (5)$$

where the subscripts exp and cal refer to the experimental and the calculated data, and n is the number of data points.

Fig. 4 displays the adsorption isotherms of Procion Red MX-5B on CNTs at 301 K (other temperatures not shown), which revealed the relationship between the amount of Procion Red MX-5B adsorbed per unit mass of CNTs (q) and the equilibrium concentration in solution (C). Table 1 summarized the coefficients of the Langmuir and Freundlich isotherms at different pH values and temperatures. Most of the R^2 values exceed 0.9 and the S.D. values are smaller than 15% for both the Langmuir and the Freundlich models, suggesting that both models closely fitted the experimental results. However, the regression results demonstrated that the Langmuir isotherm fitted the experimental data better than the Freundlich at 301 K (Fig. 4). The values of K_L at pH 6.5 were 0.56, 0.72, 0.93 and 2.98 l/mg at 281, 291, 301 and 321 K, respectively, and those at pH 10 were 0.22, 0.28, 0.65 and 1.81 l/mg at 281, 291, 301 and 321 K, respectively. K_L increased with temperature and declined as the pH increased, revealing that the adsorption of Procion Red MX-5B on CNTs dropped as the pH increased but increased with temperature. The results implied that the affinity of the binding sites for Procion Red MX-5B increased with the temperature. The saturation adsorption capacity (q_m) increased as pH decreased. The saturation adsorption capacity of Procion

Table 1
Coefficients of Langmuir and Freundlich isotherms

	Langmuir model					Freundlich model			
	K_L (l/mg)	q_m (mg/g)	R^2	R_L	S.D. (%)	K_F	n	R^2	S.D. (%)
281 K									
pH 6.5	0.56	42.92	0.939	0.08	15.4	16.39	3.49	0.972	7.8
pH 10	0.22	38.02	0.890	0.19	20.3	7.74	2.11	0.890	20.0
291 K									
pH 6.5	0.72	44.64	0.942	0.06	12.8	16.22	3.53	0.866	16.3
pH 10	0.28	42.55	0.939	0.15	8.2	15.63	3.84	0.998	11.3
301 K									
pH 6.5	0.93	39.84	0.992	0.05	13.2	16.26	3.43	0.973	13.9
pH 10	0.65	35.21	0.992	0.07	7.2	16.16	4.35	0.928	10.1
321 K									
pH 6.5	2.98	35.71	0.921	0.02	10.4	22.78	6.97	0.956	6.3
pH 10	1.81	29.94	0.809	0.03	15.5	17.93	6.01	0.918	8.8

Red MX-5B by metal hydroxide sludge [21], cross-linked chitosan beads [17], TiO_2, TiO_2/AC and TiO_2/CNTs [13] is 62.5, 2422.0, 6.3, 13.3 and 14.4 mg/g, respectively. Despite of the saturation adsorption capacity in this study (29.94–44.64 mg/g) was lower than that of metal hydroxide sludge and cross-linked chitosan beads; however, the TiO_2/CNTs composites have significantly more photocatalytic activity than TiO_2 and the TiO_2/AC composite [14]. R_L lied between zero and unity, suggesting that the adsorption of Procion Red MX-5B on CNTs was favorable.

With respect to the coefficients of the Freundlich model, K_F increased with the temperature, indicating that the adsorption capacity increased with the temperature. Like K_F, n increased with temperature. The highest value of n, 6.97 at pH 6.5 and 321 K, represents favorable adsorption at high temperature and low pH. If the n is below unity, then the adsorption is chemical; otherwise, the adsorption is physical [22]. All values of n exceeded two, suggesting that the adsorption of Procion Red MX-5B on CNTs is physical. Gemeay [18] suggested that the higher value of $1/n$ corresponded greater heterogeneity of the adsorbent surface. As shown in Table 1, the degree of heterogeneity of the CNTs surface declines as the temperature increases. Both the Langmuir and the Freundlich models suggest that increasing temperature increased adsorption capacity, revealing that the adsorption is endothermic. The following section presents the detailed thermodynamic parameters.

3.3. Kinetic and thermodynamic analyses

3.3.1. Kinetic analyses

The kinetic analysis of temperature effect was evaluated at pH 6.5 (Fig. 5). The 3 h adsorption capacity at 281, 291, 301 and 321 K was 20.93, 22.87, 27.20 and 30.53 mg/g, respectively. The adsorption increased with temperature, indicating that the mobility of dye molecules increased with temperature, as did the number of molecules that interact with the active sites at CNTs; moreover, the adsorption was endothermic. Additionally, increasing the temperature reduces the viscosity of the solution and increases the rate of diffusion of dye molecules. The adsorption is initially (contact time <1 h) rapid, and then slows (Fig. 5), perhaps because a large number of vacant surface sites were available for adsorption during the initial stage, and then, the remaining vacant surface sites were difficult to occupy because of the repulsive forces between the dye molecules on the CNTs and the bulk phase [23].

Pseudo first- and second-order models and intraparticle diffusion models were applied to test the experimental data and thus

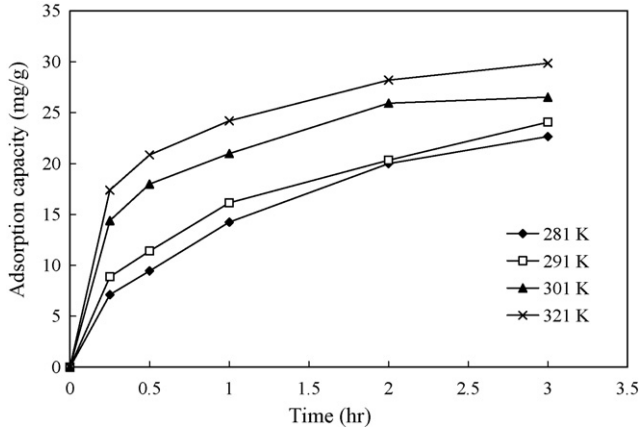

Fig. 5. Kinetic analysis of temperature effect (Procion Red MX-5B = 20 mg/l, CNTs = 0.25 g/l and pH 6.5).

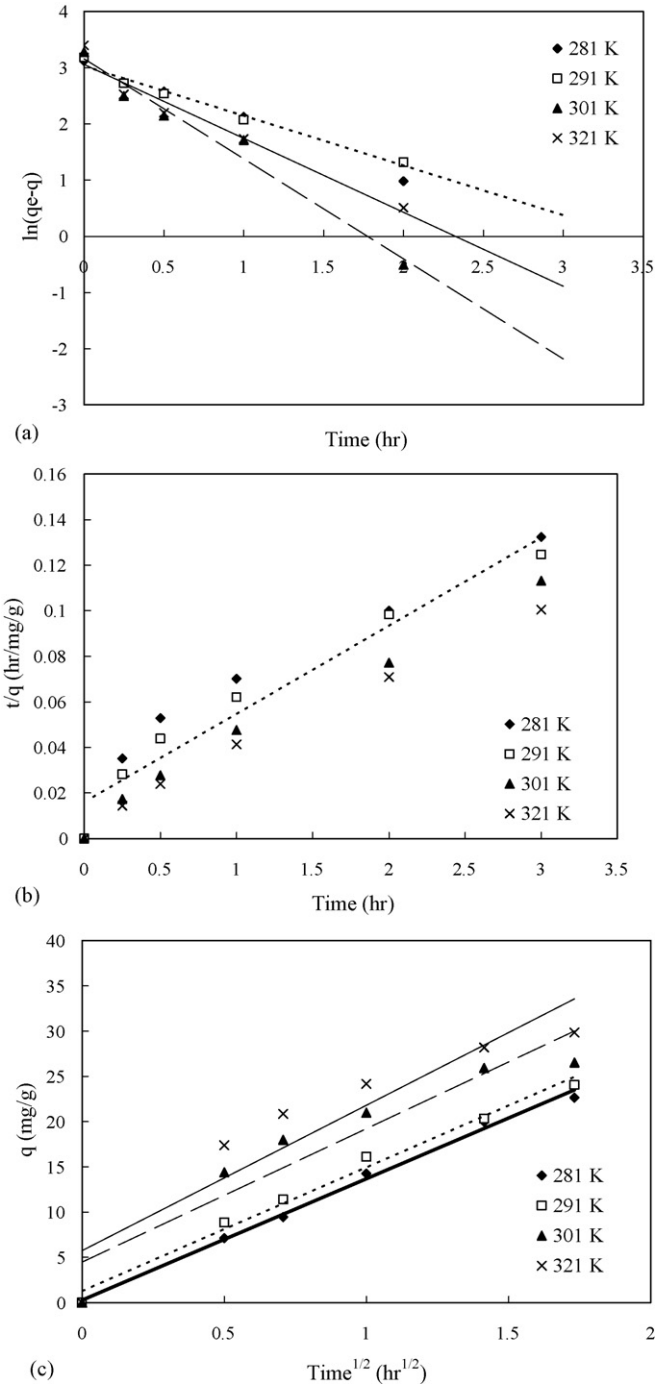

Fig. 6. Regressions of kinetic plots at different temperature: (a) pseudo first-order model, (b) pseudo second-order model and (c) intraparticle diffusion model.

elucidate the kinetic adsorption process. The pseudo first-order model can be expressed as:

$$\ln(q_e - q) = \ln(q_e) - k_1 t \quad (6)$$

where q_e and q are the amounts of Procion Red MX-5B adsorbed on CNTs at equilibrium and at various times t (mg/g) and k_1 is the rate constant of the pseudo first-order model for the adsorption (h^{-1}) [19]. The values of q_e and k_1 can be determined from the intercept and the slope of the linear plot of $\ln(q_e - q)$ versus t. The pseudo second-order model is given by:

$$\frac{t}{q} = \frac{1}{k_2 q_e^2} + \frac{t}{q_e} \quad (7)$$

where q_e and q are defined as in the pseudo first-order model; k_2 is the rate constant of the pseudo second-order model for adsorption (g/mg h) [19]. The slope and intercept of the linear plot of t/q against t yielded the values of q_e and k_2. Additionally, the initial adsorption rate h (mg/g h) can be determined from $h = k_2 q_e^2$. Since neither the pseudo first-order nor the second-order model can identify the diffusion mechanism, the kinetic results were analysed by the intraparticle diffusion model to elucidate the diffusion mechanism, which model is expressed as:

$$q = k_i t^{1/2} + C \quad (8)$$

where C is the intercept and k_i is the intraparticle diffusion rate constant (mg/g $h^{0.5}$), which can be evaluated from the slope of the linear plot of q versus $t^{1/2}$ [24].

The results of Fig. 5 are fitted using pseudo first- and second-order models and intraparticle diffusion model. Fig. 6(a)–(c) displays the linear regressions. Table 2 presented the coefficients of the pseudo first- and second-order adsorption kinetic models and the intraparticle diffusion model. The R^2 values of the pseudo first- and second-order models exceeded 0.93, but S.D. values of the pseudo second-order model were smaller than those of the pseudo first-order model. Moreover, the q values ($q_{e,cal}$) calculated from pseudo second-order model were more consistent with the experimental q values ($q_{e,exp}$) than those calculating from the pseudo first-order model. Hence, this study suggested that the pseudo second-order model better represented the adsorption kinetics. A similar phenomenon has been observed in the adsorption of Procion Red MX-5B by cross-linked chitosan beads [17], Acid Blue 93 by natural sepiolite [25], Acid Red 57 by surfactant-modified sepiolite [26], and Acid Blue 193 by both BTMA-bentonite [27] and DEDMA-sepiolite [28]. The values of k_2, h, $q_{e,exp}$ and $q_{e,cal}$ all increased with the temperature. Ozcan et al. [25] proposed that the adsorption of Acid Blue 93 by natural sepiolite proceeds by physisorption, in which increasing the temperature increases the adsorption rate but reduces adsorption capacity. However, this study suggested that the thermodynamic analyses were more appropriate for determining whether the adsorption was a physisorption or a chemisorption process, as would be discussed in the following section.

Typically, various mechanisms control the adsorption kinetics; the most limiting are the diffusion mechanisms, including external diffusion, boundary layer diffusion and intraparticle diffusion [29]. Hence, the intraparticle diffusion model was utilized to determine the rate-limiting step of the adsorption process. If the regression of q versus $t^{1/2}$ is linear and passes through the origin, then intraparticle diffusion is the sole rate-limiting step [26,30]. The regression was linear, but the plot did not pass through the origin (Fig. 6(c)), suggesting that adsorption involved intraparticle diffusion, but that was not the only rate-controlling step. Other kinetic models may control the adsorption rate, which finding is similar to that made in previous works on adsorption [25,28]. The k_i values (13.40–16.07 mg/g $h^{0.5}$) increased with the temperature (281–321 K), increasing the mobility of dye molecules. Addi-

Table 2
Coefficients of pseudo first- and second-order adsorption kinetic models and intraparticle diffusion model (dye concentration = 20 mg/l, CNTs = 0.25 g/l and pH 6.5)

Temperature (K)	$q_{e,exp}$ (mg/g)	k_1 (h^{-1})	$q_{e,cal}$ (mg/g)	R^2	S.D. (%)
Pseudo first-order model					
281	20.93	1.040	21.98	0.994	15.5
291	22.87	0.886	27.20	0.979	21.7
301	27.20	1.781	23.56	0.976	25.1
321	30.53	1.315	21.29	0.955	43.4

Temperature (K)	$q_{e,exp}$ (mg/g)	k_2 (g/mg h)	h (mg/g h)	$q_{e,cal}$ (mg/g)	R^2	S.D. (%)
Pseudo second-order model						
281	20.93	0.073	47.51	25.51	0.932	18.7
291	22.87	0.094	62.76	25.84	0.956	15.3
301	27.20	0.190	147.47	27.86	0.990	10.0
321	30.53	0.195	185.71	30.86	0.993	8.1

Temperature (K)	k_i (mg/g $h^{0.5}$)	C (mg/g)	R^2	S.D. (%)
Intraparticle diffusion model				
281	13.40	0.29	0.995	3.8
291	13.67	1.27	0.988	6.3
301	14.74	4.48	0.893	14.6
321	16.07	5.74	0.865	15.9

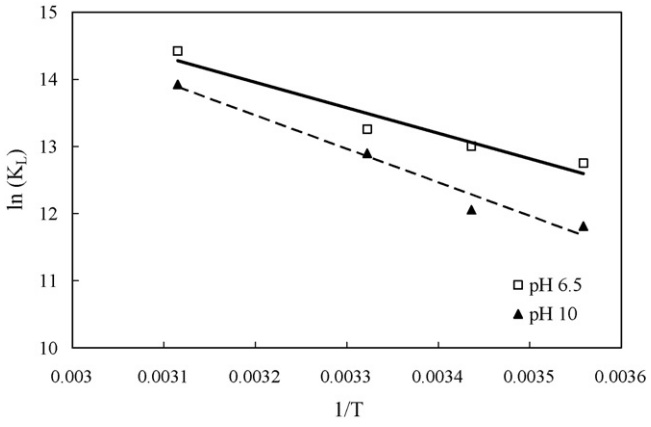

Fig. 7. Regressions of van't Hoff plot for thermodynamic parameters.

tionally, the C value (0.29–5.74 mg/g) varied like the k_i values with temperature (Table 2). The values of C are helpful in determining the boundary thickness: a larger C value corresponds to a greater boundary layer diffusion effect [30]. The results of this study demonstrated increasing the temperature promoted the boundary layer diffusion effect.

3.3.2. Thermodynamic analyses

The thermodynamic parameters provide in-depth information regarding the inherent energetic changes associated with adsorption; therefore, they should be properly evaluated. Free energy of adsorption (ΔG°), enthalpy (ΔH°), and entropy (ΔS°) changes and activation energy (E_a) were calculated in this study to predict the process of adsorption.

The Langmuir isotherm was used to calculate thermodynamic parameters using the following equations:

$$\Delta G^\circ = -RT \ln(K_L) \tag{9}$$

$$\ln(K_L) = \frac{\Delta S^\circ}{R} - \frac{\Delta H^\circ}{RT} \tag{10}$$

where K_L is the Langmuir equilibrium constant (l/mol); R the gas constant (8.314 J/mol K) and T is the temperature (K). ΔH° and ΔS° were determined from the slope and intercept of the van't Hoff plots of $\ln(K_L)$ versus $1/T$ [20,25,27,28,31]. Fig. 7 shows the van't Hoff plot for the adsorption of Procion Red MX-5B onto CNTs. Table 3 presented the thermodynamic parameters at various temperatures and pH values. The values of ΔH° and ΔS° were 31.55 kJ/mol and 216.99 J/mol K at pH 6.5 and those at pH 10 were 41.47 kJ/mol and 244.64 J/mol K, respectively (Table 3). Kara et al. [32] suggested that the ΔH° of physisorption is smaller than 40 kJ/mol. Based on ΔH°, this study suggested that the adsorption of Procion Red MX-5B onto CNTs was a physisorption process. Positive ΔH° and ΔS° values suggest that the adsorption of Procion Red MX-5B onto CNTs is endothermic, which fact is supported by the increase in the adsorption of Procion Red MX-5B with temperature. Moreover, the positive ΔS° indicated that the degrees of freedom increased at the solid–liquid interface during the adsorption of Procion Red MX-5B onto CNTs. The ΔG° values were negative at all of the tested pHs (6.5 and 10) and temperatures (281–321 K), confirming that the adsorption of Procion Red MX-5B onto CNTs was spontaneous and thermodynamically favorable. Restated, a more negative ΔG° implied a greater driving force of adsorption, resulting in a higher adsorption capacity. When the temperature increased from 281 to 321 K, ΔG° became a high negative value, suggesting that adsorption was more spontaneous at high temperature. The adsorption was more spontaneous at low pH than at high pH. Generally, ΔG° for physisorption is less than that for chemisorption. The former is between −20 and 0 kJ/mol and the latter is between −80 and −400 kJ/mol [33]. Therefore, the ΔG° results implied that physisorption might dominate the adsorption of Procion Red MX-5B onto CNTs.

Table 3
Thermodynamic parameters at various temperatures and pHs

	ΔG° (kJ/mol)	ΔH° (kJ/mol)	E_a (kJ/mol)	ΔS° (J/mol K)
pH 6.5				
281 K	−29.79	31.55	33.35	216.99
291 K	−31.45			
301 K	−33.18			
321 K	−38.49			
pH 10				
281 K	−27.60	41.47	–	244.64
291 K	−29.17			
301 K	−32.28			
321 K	−37.16			

The pseudo second-order model was identified as the best kinetic model for the adsorption of Procion Red MX-5B onto CNTs. Accordingly, the rate constants (k_2) of the pseudo second-order model were adopted to calculate the activation energy of the adsorption process using the Arrhenius equation [34]:

$$\ln(k_2) = \ln(A) - \frac{E_a}{RT} \tag{11}$$

where k_2, A, E_a, R and T are the rate constant of the pseudo second-order model (g/mg h), the Arrhenius factor, the activation energy (kJ/mol), the gas constant (8.314 J/mol K) and the temperature (K), respectively. The activation energy could be determined from the slope of the plot of $\ln(k_2)$ versus $1/T$. The activation energy was 33.35 kJ/mol at pH 6.5 (Table 3). The magnitude of the activation energy yields information on whether the adsorption is mainly physical or chemical. Nollet et al. [31] suggested that the physisorption process normally had activation energy of 5–40 kJ/mol, while chemisorption had a higher activation energy (40–800 kJ/mol). Therefore, ΔH°, ΔG° and E_a all suggested the same fact: the adsorption of Procion Red MX-5B onto CNTs was a physisorption process. Lazaridis and Asouhidou [35] stated that in a diffusion-controlled process, the activation energy of adsorption was less than 25–30 kJ/mol. Based on the results of activation energy and the intraparticle diffusion model (Table 3 and Fig. 6(c)), this study proposed that the adsorption involved intraparticle diffusion, that was not the only rate-controlling step, and the other kinetic models might control the adsorption rate.

4. Conclusion

This investigation examined the equilibrium and the dynamic adsorption of Procion Red MX-5B onto CNTs at various pHs and temperatures. The adsorption capacity was highest when 0.25 g/l CNTs was added. K_L increased with temperature and declined as the pH increased. The results suggested that the adsorption of Procion Red MX-5B on CNTs decreased as the pH rose but increased with temperature. R_L lied between zero and unity, revealing that the adsorption of Procion Red MX-5B on CNTs was favorable. The values of k_2, h, $q_{e,exp}$ and $q_{e,cal}$ all increased with the temperature, suggesting that increasing the temperature increased the adsorption capacity and the adsorption rate. The regression results of the intraparticle diffusion model suggested that intraparticle diffusion was not the only rate-controlling step. Positive ΔH° and ΔS° values indicated that the adsorption of Procion Red MX-5B onto CNTs was endothermic, which result was supported by the increasing adsorption of Procion Red MX-5B with temperature. The values of ΔH°, ΔG° and E_a all suggested that the adsorption of Procion Red MX-5B onto CNTs was a physisorption process and was spontaneous.

Acknowledgements

The authors would like to thank the National Science Council of the Republic of China for financially supporting this research under Contract no. NSC 94-2211-E-212-012. Additionally, the partial experiments of this research by Shu-Hui Kuo of National Yunlin University of Science and Technology were greatly appreciated.

References

[1] R.Q. Long, R.T. Yang, Carbon nanotubes as superior sorbent for dioxin removal, J. Am. Chem. Soc. 123 (2001) 2058–2059.
[2] C.S. Lu, H.S. Chiu, Adsorption of zinc(II) from water with purified carbon nanotubes, Chem. Eng. Sci. 61 (2006) 138–145.
[3] Y.H. Li, S. Wang, Z. Luan, J. Ding, C. Xu, D. Wu, Adsorption of cadmium(II) from aqueous solution by surface oxidized carbon nanotubes, Carbon 41 (2003) 1057–1062.
[4] Y.H. Li, S.G. Wang, J.Q. Wei, X.F. Zhang, C.L. Xu, Z.K. Luan, D.H. Wu, B.Q. Wei, Lead adsorption on carbon nanotubes, Chem. Phys. Lett. 357 (2002) 263–266.
[5] Y.H. Li, Z. Di, J. Ding, D. Wu, Z. Luan, Y. Zhu, Adsorption thermodynamic, kinetic and desorption studies of Pb^{2+} on carbon nanotubes, Water Res. 39 (2005) 605–609.
[6] Y.H. Li, Y. Zhu, Y. Zhao, D. Wu, Z. Luan, Different morphologies of carbon nanotubes effect on the lead removal from aqueous solution, Diam. Relat. Mater. 15 (2006) 90–94.
[7] X. Peng, Z. Luan, Z. Di, Z. Zhang, C. Zhu, Carbon nanotubes-iron oxides magnetic composites as adsorbent for removal of Pb(II) and Cu(II) from water, Carbon 43 (2005) 880–883.
[8] Z.C. Di, J. Ding, X.J. Peng, Y.H. Li, Z.K. Luan, J. Liang, Chromium adsorption by aligned carbon nanotubes supported ceria nanoparticles, Chemosphere 62 (2006) 861–865.
[9] Y.H. Li, S. Wang, X. Zhang, J. Wei, C. Xu, Z. Luan, D. Wu, Adsorption of fluoride from water by aligned carbon nanotubes, Mater. Res. Bull. 38 (2003) 469–476.
[10] X. Peng, Z. Luan, J. Ding, Z. Di, Y. Li, B. Tian, Ceria nanoparticles supported on carbon nanotubes for the removal of arsenate from water, Mater. Lett. 59 (2005) 399–403.
[11] C.S. Lu, Y.L. Chung, K.F. Chang, Adsorption of trihalomethanes from water with carbontubes, Water Res. 39 (2005) 1183–1189.
[12] X. Peng, Y. Li, Z. Luan, Z. Di, H. Wang, B. Tian, Z. Jia, Adsorption of 1,2-dichlorobenzeze from water to carbon nanotubes, Chem. Phys. Lett. 376 (2003) 154–158.
[13] Y. Yu, J.C. Yu, C.Y. Chan, Y.K. Che, J.C. Zhao, L. Ding, W.K. Ge, P.K. Wong, Enhancement of adsorption and photocatalytic activity of TiO_2 by using carbon nanotubes for the treatment of azo dye, Appl. Catal. B: Environ. 61 (2005) 1–11.
[14] Y. Yu, J.C. Yu, J.G. Yu, Y.C. Kwok, Y.K. Che, J.C. Zhao, L. Ding, W.K. Ge, P.K. Wong, Enhancement of photocatalytic activity of mesoporous TiO_2 by using carbon nanotubes, Appl. Catal. A: Gen. 289 (2005) 186–196.
[15] K.G. Bhattacharyya, A. Sharma, Kinetics and thermodynamics of Methylene Blue adsorption on Neem (*Azadirachta indica*) leaf powder, Dyes Pigments 65 (2005) 51–59.
[16] K. Marungrueng, P. Pavasant, Removal of basic dye (Astrazon Blue FGRL) using macroalga *Caulerpa lentillifera*, J. Environ. Manage. 78 (2006) 268–274.
[17] M.S. Chiou, P.Y. Ho, H.Y. Li, Adsorption of anionic dyes in acid solutions using chemically cross-linked chitosan beads, Dyes Pigments 60 (2004) 69–84.
[18] A.H. Gemeay, Adsorption characteristics and kinetics of the cation exchange of rhodamine-6G with Na^+-montmorillonite, J. Colloid Interf. Sci. 251 (2002) 235–241.
[19] Y.S. Ho, G. McKay, Sorption of dye from aqueous solution by pit, Chem. Eng. J. 70 (1998) 115–124.
[20] A.S. Ozcan, B. Erdem, A. Ozcan, Adsorption of Acid Blue 193 from aqueous solutions onto Na-bentonite and DTMA-bentonite, J. Colloid Interf. Sci. 280 (2004) 44–54.
[21] S. Netpradit, P. Thiraretyan, S. Towprayoon, Application of "waste" metal hydroxide sludge for adsorption of azo reactive dyes, Water Res. 37 (2003) 763–772.
[22] J.Q. Jiang, C. Cooper, S. Ouki, Comparison of modified montmorillonite adsorbents. Part I: Preparation, characterization and phenol adsorption, Chemosphere 47 (2002) 711–716.
[23] I.D. Mall, V.C. Srivastava, N.K. Agarwal, Removal of Orange-G and Methyl Violet dyes by adsorption onto bagasse fly ash—kinetic study and equilibrium isotherm analyses, Dyes Pigments 69 (2006) 210–223.
[24] W.J. Weber Jr., J.C. Morris, Kinetics of adsorption on carbon from solution, J. Sanit. Eng. Div. 89 (1963) 31–59.
[25] A. Ozcan, E.M. Oncu, A.S. Ozcan, Kinetics, isotherm and thermodynamic studies of adsorption of Acid Blue 193 from aqueous solutions onto natural sepiolite, Colloid Surf. A 277 (2006) 90–97.
[26] A. Ozcan, A.S. Ozcan, Adsorption of Acid Red 57 from aqueous solutions onto surfactant-modified sepiolite, J. Hazard. Mater. 125 (2005) 252–259.
[27] A.S. Ozcan, B. Erdem, A. Ozcan, Adsorption of Acid Blue 193 from aqueous solutions onto BTMA-bentonite, Colloid Surf. A 266 (2005) 73–81.
[28] A. Ozcan, E.M. Oncu, A.S. Ozcan, Adsorption of Acid Blue 193 from aqueous solutions onto DEDMA-sepiolite, J. Hazard. Mater. 129 (2006) 244–252.
[29] E. Guibal, P. McCarrick, J.M. Tobin, Comparison of the sorption of anionic dyes on activated carbon and chitosan derivatives from dilute solutions, Sep. Sci. Technol. 38 (2003) 3049–3073.
[30] K. Kannan, M.M. Sundaram, Kinetics and mechanism of removal of Methylene Blue by adsorption on various carbons—a comparative study, Dyes Pigments 51 (2001) 25–40.
[31] H. Nollet, M. Roels, P. Lutgen, P. Meeren, W. Verstraete, Removal of PCBs from wastewater using fly ash, Chemosphere 53 (2003) 655–665.
[32] M. Kara, H. Yuzer, E. Sabah, M.S. Celik, Adsorption of cobalt from aqueous solutions onto sepiolite, Water Res. 37 (2003) 224–232.
[33] M.J. Jaycock, G.D. Parfitt, Chemistry of Interfaces, Ellis Horwood Ltd., Onichester, 1981, pp. 12–13.
[34] M. Dogan, M. Alkan, Adsorption kinetics of Methyl Violet onto perlite, Chemosphere 50 (2003) 517–528.
[35] N.K. Lazaridis, D.D. Asouhidou, Kinetics of sorptive removal of chromium(VI) from aqueous solutions by calcined Mg–Al–COB_3 hydrotalcite, Water Res. 37 (2003) 2875–2882.